Lubricant Characterization by Molecular Simulation

J. D. Moore, S. T. Cui, P. T. Cummings, and H. D. Cochran
Dept. of Chemical Engineering, University of Tennessee, Knoxville, TN 37996
Chemical Technology Div., Oak Ridge National Laboratory, Oak Ridge, TN 37831

Lubrication is a phenomenon of immense practical importance and fundamental scientific interest, and the automobile engines of the future are envisioned by the Partnership for a New Generation Vehicle will require the development of improved lubricants that perform well at higher operating temperatures and higher engine speeds. The rheological properties of liquid alkanes of intermediate molecular sizes (C20H42-C40H82) are among the most important properties in lubricant performance. Though realistic study of these systems by molecular simulation has previously been limited by both high computational costs and the lack of potential models accurate over a wide range of physical conditions, the advent of massively parallel supercomputers has now made such studies possible. As an illustration of the ability of molecular simulation as a useful tool for lubricant development, we present the first molecular-simulation-based calculation of the kinematic viscosity index of an alkane liquid, viz. 2,6,10,15, 19,23-hexamethytetracosane, commonly called squalane. In the mass range of interest, squalane is one of the few commercially available isoparaffins and has been the subject of previous studies by molecular simulation (Mondello and Grest 1995; Mundy et al., 1997).

Though numerous properties of a lubricant are important to end-use applications, the viscosity is considered most significant. Mundy et al. (1996) investigated the variation of decane's viscosity with pressure, calculating its pressure-viscosity coefficient by equilibrium molecular dynamics simulations. The kinematic viscosity index (VI) is another widely-used industrial characterization of automotive lubricants. It was proposed by Dean and Davis (1929) as an indication of an oil's viscosity-temperature characteristics in terms of its Saybolt viscosities at 311 K (100°F) and 372 K (210°F). Two series of reference lubricating-oil fractions (H and L) were used for comparison. Series H exhibited little change of viscosity with temperature while the viscosities of series L oils exhibited large variation with temperature. Series H and L represented, respectively, the best and worst oils available in 1929. Series H oils were assigned a VI of 100, series L a value of 0. The VI of an oil under test (T) was calculated from the equation

$$\mathrm{VI} = \frac{L - U}{L - H} \times 100$$

where U is the kinematic viscosity at 311 K of the oil in question, L and H, respectively, are the kinematic viscosities at 311 K of the series L and H having the same kinematic viscosity at 372 K as the oil T. Thus, the higher the VI the less the viscosity of an oil is affected by temperature and, therefore, the better the oil. Subsequently, Hardiman and Nissan (1945) proposed revision to the VI system because it had reached the end of usefulness in its previous form. It had become necessary to give VI values to oils with better viscosity-temperature behavior than those represented by 100 on the VI scale. Hardiman and Nissan found that the VI system failed for viscosity indices greater than 130, and comparison became meaningless. Hardiman and Nissan sought to make the VI applicable at any two temperatures and to a wider range of oils. They reported the following empirical equations for the VI

$$\mathrm{VI} = 3.63[60 - 10^{n}] \tag{1}$$

where n is given by

$$n = \frac{\log \nu_1 - \log k}{\log \nu_2} \tag{2}$$

Equation 2 is a rearrangement of the equation

$$\nu_1 = k \cdot \nu_2^{n}$$

where ν_1 is the kinematic viscosity in cSt at the lower temperature, ν_2 is the kinematic viscosity in cSt at the higher temperature, k is a function of the temperature range alone and is independent of the nature of the oil, and n, a constant characteristic for each oil, depends on the temperature range

Correspondence concerning this article should be addressed to P. T. Cummings.

chosen. For the temperature range 311–372 K, Hardiman and Nissan determined k to be 2.714. They found good correlation between their suggested VI and that of Dean and Davis, theirs having the advantage of applicability to a wider range of oils. Though used subsequently in standard data compilations, such as that of Dixon et al. (1966), the VI as defined by Hardiman and Nissan did not become the ASTM standard. Based on the kinematic viscosity of the oil at 313 K and 373 K, the present standard (ASTM D2270-93) is identical to that of Dean and Davis for oils with VI less than 100. A different formula, similar to the one proposed by Hardiman and Nissan, is used for oils with VI greater than 100.

Utilizing the united atom model for alkanes previously used by Siepmann et al. (1993); Smit et al. (1995) and Mondello and Grest (1995), and rRESPA multitimestep dynamics (Tuckerman et al., 1992; Mundy et al., 1995; Cui et al., 1996), we calculate on the Intel Paragon massively parallel supercomputers the shear-rate-dependent viscosity of squalane for strain rates ranging over several orders of magnitude at the two temperatures. The low strain rate (Newtonian) values of the viscosity are used to calculate the kinematic viscosity index.

Simulation Methodology

The equations of motion used to simulate squalane under planar Couette flow are the SLLOD equations (Evans and Morris, 1990) (incorporating a Nosé thermostat),

$$\dot{r}_{ia} = \frac{p_{ia}}{m_{ia}} + \gamma y_{ia}\hat{x}$$

$$\dot{p}_{ia} = F_{ia} - \gamma p_{y,ia}\hat{x} - \dot{\zeta} p_{ia}$$

$$\dot{\zeta} = \frac{p_\zeta}{Q}$$

$$\dot{p}_\zeta = F_\zeta,$$

where r_{ia}, F_{ia}, and p_{ia} are the coordinates of, force on, and momentum of atom a in molecule i, y_{ia} and $p_{y,ia}$ are its y components, and m_{ia} is the mass. The strain rate of the imposed shear field is denoted γ, $\hat{x}$ is a unit vector in the x direction, ζ, p_ζ, and Q are the variables related to the Nosé thermostat

$$F_\zeta = \sum_{ia} \frac{p_{ia}}{m_{ia}} - 3Nk_BT, \quad Q = 3Nk_BT\tau^2$$

τ is the Nosé thermostat time constant, k_B is Boltzmann's constant, T is the absolute temperature, and N is the total number of atoms in the system.

In a nonequilibrium molecular dynamics (NEMD) calculation, the shear-rate dependent viscosity η is determined from the constitutive relation

$$\eta = -\frac{\langle P_{xy}\rangle + \langle P_{yx}\rangle}{2\gamma}$$

where $\langle P_{xy}\rangle$ and $\langle P_{yx}\rangle$ are the averages of the xy and yx components of the pressure tensor P and γ is the strain rate characterizing the shear field. We have chosen the x direction to be the flow direction and the y direction to be the flow gradient direction, so that $\gamma = \partial u_x/\partial y$ where u_x is the streaming velocity in the x direction.

The model used for squalane is the united atom model for alkanes previously used by Siepmann et al. (1993), Smit et al. (1995), and Mondello and Grest (1995). The methyl and methylene groups are treated as spherical interaction sites with interaction centers located at the centers of the carbon atoms. The interaction between atoms on different molecules and atoms separated by more than three bonds in the same molecule is described by the well-known Lennard-Jones (LJ) potential with a cut-off distance of $2.5\sigma_{CH_2}$. The intramolecular interactions include a stretching term, a bending term, and a torsional term. The bond stretching is described by a harmonic potential (Mundy et al., 1995) with an equilibrium bond distance of 1.54 Å and a force constant $A/k_B = 452{,}900$ K/Å^2. The bond bending interaction is described by a harmonic potential with an equilibrium angle of $\theta = 114°$ and a force constant of $A/k_B = 62{,}500$ K/rad^2. The torsional interaction is described by the potential developed by Jorgensen et al. (1984). To prevent umbrella inversion of the sp_3 bond configuration at tertiary carbon branch points, we use a harmonic potential similar to the bending term introduced by Mondello and Grest (1995). The LJ size and energy parameters and the intramolecular interaction parameters can be found in Mondello and Grest (1995).

The equations of motion were integrated using a multiple time step technique with Nosé constant temperature dynamics, the details of which can be found in the works of Tuckerman et al. (1992) and Cui et al. (1996). Two time step sizes of 2.35 fs and 0.47 fs were used. All the internal interactions were treated as fast motions (smaller time step) and the intermolecular interaction as the slow motion (larger time step). The configuration of a neighboring higher strain rate was used as the starting configuration for the next smaller strain rate as this allows the system to reach steady state more quickly than starting from an equilibrium configuration. At each strain rate, after allowing 0.235 ns for the system to reach steady state, the strain rate dependent properties were calculated based on a simulation run of length varying from 0.987 ns at the highest strain rate to 16.2 ns at the lowest strain rate and lower temperature. The computational investment for this calculation totaled approximately 125,000 node hours on the Intel Paragon.

Results

In Figure 1, the kinematic viscosity ($\nu = \eta/\rho$, where ρ is density) of squalane is plotted at the state points $T = 311$ K and $T = 372$ K as a function of strain rate. These state points correspond to the experimental equilibrium density at atmospheric pressure at the respective temperatures. The figure is plotted on a log-log scale and covers several orders of magnitude. The dashed lines indicate the Newtonian (zero shear-rate) experimental results, and the arrows indicate the independently predicted transition between Newtonian and non-Newtonian behavior (inverse of the rotational relaxation times reported by Mondello and Grest (1995)). Detailed numerical data and production run lengths are tabulated in Table 1. As can be seen from the figure, the viscosity shows shear thin-

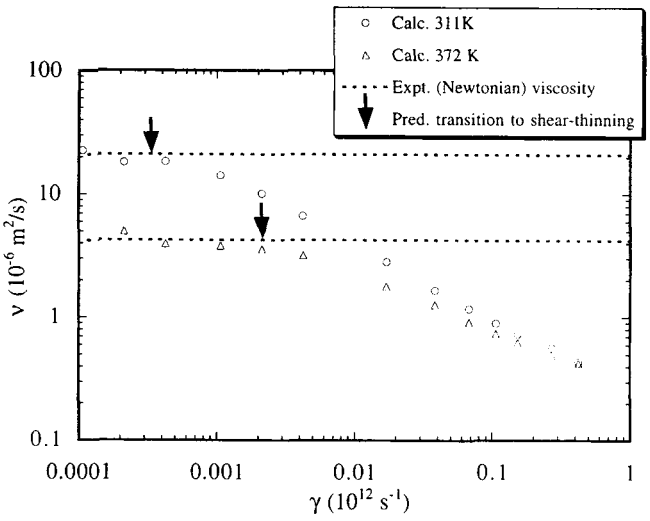

Figure 1. Kinematic viscosity of squalane as a function of strain rate at 311 K and 372 K.

ning behavior as a function of strain rate, as is typically observed in chain molecule systems. This shear thinning seen at high strain rates is characteristic of the conditions in critical lubrication applications such as automotive engine cam-shaft lifters ($\sim 10^8$ s^{-1}), which are at strain rates well above those where the viscosity can be measured experimentally. At lower strain rates, the viscosity vs. strain rate curves approach the experimental Newtonian values as reported by Dixon et al. (1966).

Two methods for evaluating the Newtonian viscosity from the NEMD simulation results were considered and are summarized in Table 2. In the first method, the kinematic viscosity at 311 K (19.7 ± 2.1 cSt) was computed as the average of the three lowest strain rate values and the kinematic viscosity at 372 K (4.06 ± 0.55 cSt) was computed as the average of the four lowest strain rate values, yielding via the current ASTM standard a VI of 115 ± 70 by a standard propagation of errors. In the second method, the lowest strain rate values were ignored. Thus, the kinematic viscosity at 311 K (18.2 ± 0.1 cSt) was computed as the average of the second and third lowest strain rate values and the kinematic viscosity at 372 K (3.75 ± 0.16 cSt) was computed as the average of the second, third and fourth lowest strain rate values, yielding a VI of 103 ± 18 by standard propagation of errors. Although the error in the experimental viscosities is not reported in API 42 (Dixon et al., 1966), a reasonable upper bound is 5%; the error in the experimental VI (116 ± 30 cSt) that results in this case from standard propagation of errors is given in Table 2. Whichever method is used to calculate the VI from the NEMD data, it is clear that the result from NEMD simulation is in very good agreement with the experimental measurement.

Table 1. Kinematic Viscosity of Squalane as a Function of Strain Rate*

Strain Rate (s^{-1})	Reduced Strain Rate $\gamma(m\sigma^2/\epsilon)^{1/2}$	Squalane 311 K: Kinematic Viscosity (10^{-6} m^2/s)	Squalane 311 K: Run Length (ns)	Squalane 372 K: Kinematic Viscosity (10^{-6} m^2/s)	Squalane 372 K: Run Length (ns)
1.063×10^8	0.00025	22.7 (66)	17.4		
2.126×10^8	0.0005	18.1 (28)	9.35	5.41 (164)	7.26
4.251×10^8	0.001	18.3 (17)	7.00	3.93 (48)	4.61
1.063×10^9	0.0025	14.1 (4)	2.14	3.79 (46)	4.47
2.126×10^9	0.005	10.1 (2)	2.70	3.55 (13)	5.41
4.251×10^9	0.01	6.64 (20)	1.67	3.16 (9)	3.45
1.700×10^{10}	0.04	2.81 (5)	1.29	1.77 (7)	1.55
3.826×10^{10}	0.09	1.64 (1)	0.94	1.25 (1)	1.46
6.802×10^{10}	0.16	1.16 (1)	1.18	0.911 (6)	1.27
1.063×10^{11}	0.25	0.899 (9)	1.18	0.744 (7)	1.79
1.5307×10^{11}	0.36	0.735 (3)	1.20	0.629 (4)	1.08
2.721×10^{11}	0.64	0.570 (3)	1.01	0.497 (2)	1.08
4.251×10^{11}	1.00	0.439 (2)	0.99	0.429 (2)	0.99

*Numbers in the parentheses represent the statistical uncertainty in the least significant digits.

Table 2. Calculation of Kinematic Viscosity Index with Error Estimates Based on Several Different Scenarios

Source	Kinematic Viscosity (10^{-6} m^2/s): 311 K	Kinematic Viscosity (10^{-6} m^2/s): 372 K	Kinematic Viscosity Index
Experiment*	20.9 ± 1.0	4.22 ± 0.21	116 ± 30
NEMD**	19.7 ± 2.1	4.06 ± 0.55	115 ± 70
NEMD†	18.2 ± 0.1	3.75 ± 0.16	103 ± 18

*Based on assuming a 5% error in the experimental measurements.
**Average of the three lowest strain rate values at 311 K and the four lowest strain rate values at 372 K.
†Average of the second and third lowest strain rate values at 311 K and the second, third and fourth lowest strain rate values of 372 K.

Conclusions

We have reported the calculation of the kinematic viscosity index of squalane from nonequilibrium molecular dynamics simulations. This represents the first accurate quantitative prediction of this measure of lubricant performance by molecular simulation. Using the same general alkane potential model, this computational approach offers the possibility of predicting the performance of potential lubricants prior to synthesis. Consequently, molecular simulation is poised to become an important tool for future lubricant development.

Acknowledgments

The work of J. D. Moore has been supported in part by a National Science Foundation Graduate Fellowship. The work of H. D. Cochran and P. T. Cummings has been supported in part by the Division of Chemical Sciences of the U.S. Dept. of Energy (DOE) at Oak Ridge National Laboratory (ORNL). The authors acknowledge the use of the Intel Paragon supercomputers in the Center for Computational Sciences at ORNL, funded by the DOE's Mathematical, Information, and Computational Sciences Division. ORNL is managed by Lockheed Martin Energy Research Corp. for the DOE under Contract No. DE-AC05-96OR22464.

Literature Cited

Cui, S. T., P. T. Cummings, and H. D. Cochran, "Multiple Time Step Nonequilibrium Molecular Dynamics Simulations of the Rheological Properties of Liquid *N*-Decane," *J. Chem. Phys.*, **104**, 255 (1996).

Dean, E. W., and G. H. B. Davis, "Viscosity Variations of Oils with Temperature," *Chem. & Met. Eng.*, **36**, 618 (1929).

Dixon, J. A., et al., "Properties of Hydrocarbons of High Molecular Weight," API 42, Amer. Pet. Inst., Res. Project 42, Washington, DC (1966).

Evans, D. J., and G. P. Morris, *Statistical Mechanics of Nonequilibrium Liquids*, Academic Press, New York (1990).
Hardiman, E. W., and A. H. Nissan, "A Rational Basis for the Viscosity Index System: I," *J. Inst. Pet.*, **31**, 255 (1945).
Jorgensen, W. L., J. D. Madura, and C. J. Swenson, "Optimized Intermolecular Potential Functions for Liquid Hydrocarbons," *J. Amer. Chem. Soc.*, **106**, 6638 (1984).
Mondello, M., and G. S. Grest, "Molecular Dynamics of Linear and Branched Alkanes," *J. Chem. Phys.*, **103**, 7156 (1995).
Mundy, C. J., J. I. Siepmann, and M. L. Klein, "Calculation of the Shear Viscosity of Decane Using a Reversible Multiple Time-Step Algorithm," *J. Chem. Phys.*, **102**, 3376 (1995).
Mundy, C. J., J. I. Siepmann, and M. K. Klein, "Decane Under Shear: A Molecular Dynamics Study Using Reversible NVT-SLLOD and NPT-SLLOD Algorithms," *J. Chem. Phys.*, **103**, 10192 (1995).
Mundy, C. J., M. L. Klein, and J. I. Siepmann, "Determination of the Pressure-Viscosity Coefficient of Decane by Molecular Simulation," *J. Phys. Chem.*, **101**, 16779 (1996).
Mundy, C. J., S. Balasubramanian, K. Bagchi, M. L. Klein, and J. I. Siepmann, *Farad. Discuss.*, **104**, 17 (1997).
Siepmann, J. I., S. Karaborni, and B. Smit, "Simulating the Critical Behavior of Complex Liquids," *Nature*, **365**, 330 (1993).
Smit, B., S. Karaborni, and J. I. Siepmann, "Computer Simulations of Vapor-Liquid Phase Equilibria of *N*-Alkanes," *J. Chem. Phys.*, **102**, 2126 (1995).
Tuckerman, M. E., B. J. Berne, and G. J. Martyna, "Reversible Multiple Time Scale Molecular Dynamics," *J. Chem. Phys.*, **97**, 1990 (1992).

Manuscript received Mar. 12, 1997, and revision received July 28, 1997.